International Journal of Research in Engineering and Science (IJRES)
ISSN (Online): 2320-9364, ISSN (Print): 2320-9356
www.ijres.org Volume 11 Issue 10 ǁ October 2023 ǁ PP. 456-464

Joule effect of *Au*-nanofluid on Cattaneo-Christovmodel along horizontal cylinder

Fareeha Tariq*, Zaffer Elahi†, Azeem Shahzad‡

Abstract
This study delves into the intricacies of heat transfer dynamics pertaining to Au nanofluid flow enveloping a horizontal stretched cylinder. Employing a judicious appli- cation of mathematical transformations, we transmute the governing partial differential equations into a set of intricate nonlinear ordinary differential equations, subsequently addressed via the formidable numerical solver, BVP4C. The fruits of our analytical la- bor are laid bare, manifesting both graphically and numerically, leveraging the prowess of the BVP4C framework. Through the prism of visual representation, we unfurl the nuanced interplay of physical parameters on the temperature profile. In addition, we quantify and present the surface-bound shear-stress rate and heat transfer rate, com- prehensively tabulated within the confines of Tables 3-4.
Keywords: *Au-nanofluid; Cattaneo-Christov model; Joule Heating Effect*

Date of Submission: 18-10-2023 Date of acceptance: 02-11-2023

I. Introduction

The Cattaneo-Christov model, a groundbreaking development in the realm of heat con- duction theory, represents a revolutionary departure from conventional Fourier's law. This model is predicated on the premise that heat propagation in a medium exhibits a finite speed, introducing the concept of thermal relaxation. Unlike the classical Fourier's law, which instantaneously propagates heat throughout a material upon a temperature dis- turbance, the Cattaneo-Christov model accounts for a finite delay in heat propagation, reflecting the time required for the heat to disperse [1] .

This model has found widespread applicability in diverse fields, from thermal engineer- ing to fluid dynamics, where fast and accurate assessments of heat transfer are paramount. By introducing the concept of thermal relaxation time, λ_1, into the heat flux equation, this model offers a more nuanced understanding of transient heat conduction phenomena.In this exploration, we delve into the intricate realm of heat transfer, an indispensable pro- cess in various engineering arenas. This phenomenon carries immense significance across

*tariqfareeha143@gmail.com, Department of Basic Sciences, University of Engineering and Technology,Taxila -47050, Pakistan,
†zaffer.elahi@uettaxila.edu.pk, Department of Basic Sciences, University of Engineering and Technology,Taxila -47050, Pakistan,
‡azeem.shahzad@uettaxila.edu.pk, Department of Basic Sciences, University of Engineering and Technol-ogy, Taxila -47050, Pakistan.

diverse applications, ranging from the cooling of nuclear reactors to the operation of heat exchangers, refrigeration systems, air coolers, and energy generation [1]. While the classical Fourier's law of heat conduction, championed by Fourier himself, has been instrumental in describing heat transfer in a multitude of experimental setups, it possesses a fundamental drawback. This model presupposes instantaneous heat propagation throughout a substance when subjected to a temperature disturbance, resulting in a parabolic equation. Recogniz- ing this limitation, Cattaneo introduced a groundbreaking modification to Fourier's law. By introducing a thermal relaxation time parameter, this alteration gave rise to a hyperbolic equation that accounts for the finite speed of heat transfer within a medium [2]. Building upon this innovation, Christov further refined the model by amalgamating Cattaneo's con- cept with Oldroyd's upper convected derivative, culminating in a material-invariant formu- lation [3]. Subsequent research endeavors have explored and applied the Cattaneo-Christov model in diverse contexts, ranging from the analysis of thermal convection in horizontal layers of incompressible Newtonian fluids [4] to investigations into structural stability and uniqueness [5], to examinations of heat transfer in viscoelastic fluids [7], nanofluid boundary layer flows [8], and magnetohydrodynamic flows over stretching sheets [9].

Furthermore, the study of flow and heat transfer in non-Newtonian fluids across stretch- ing surfaces has emerged as a prominent area of interest, particularly in engineering domains like the production of plastic and rubber sheets, hot rolling, continuous cooling, fiber spin- ning, lubrication, and suspension solutions. This research thrust has led to groundbreaking work, such as the analysis of magnetohydrodynamic axisymmetric flows [13], the exploration of heat transfer in boundary layer flows with radiative heat transfer [14], and investigations into unsteady axisymmetric flows with time-dependent stretching sheets [15].

In recent decades, the realm of micro/nano heat transfer has taken center stage. Tradi- tional fluids have long been employed to enhance heat transfer in industries like electronics, aerospace, telecommunications, biomedicine, and automotive engineering. However, the emergence of nanofluids, characterized by their superior thermal behavior and thermo- physical properties, has sparked a revolution. These nanofluids, compared to conventional coolants, not only offer enhanced performance but also contribute to environmental sus- tainability and energy conservation. Researchers have diligently explored their potential, delving into various aspects such as the effect of magnetic dipoles on energy transfer [17], mass transport mechanisms in magnetohydrodynamic spinning flows [18], and heat trans- mission in hybrid nanofluid surfaces [19]. These endeavors have provided invaluable insights into harnessing nanofluids for improved thermal management.

In light of this extensive research landscape, our study embarks on an analysis of heat transfer over a horizontally stretching cylinder in an unsteady state. To tackle this com- plex problem, we employ the Cattaneo-Christov model to formulate the energy equations. Numerical solutions are then obtained utilizing the bvp4c function to address the governing physical challenges. Our presentation of the results includes graphical representations of temperature fields, accompanied by meticulous physical justifications. Through this work, we contribute to the ever-evolving understanding of heat transfer processes and their myriad applications in engineering and industrial contexts.

II. Mathematical Formulation

Contemplate a scenario involving a two-dimensional, unidirectional, time-varying flow of incompressible, electrically conductive Au nanofluid over a stretched cylinder characterized by a radius denoted as R. This scenario is further influenced by the presence of a magnetic field, expressed as magnetic field intensity B_0. Within this configuration, we establish a coordinate system delineated by the (z, r)-axes, where z aligns with the cylinder’s axial direction, while r spans its radial extent, adhering to the conventions of cylindrical polar coordinates. Notably, this intricate fluid dynamic scenario encapsulates a heat transfer phenomenon, which we dissect with meticulous consideration of several pivotal factors. These include the incorporation of nonlinear Joule heating, the Cattaneo–Christov heat flux model, and the imposition of thermal convective boundary conditions. Figure 1 provides a visual depiction of this complex interplay.

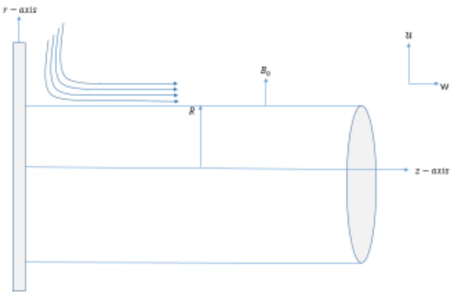

Figure 1: Geometrical view of the problem

Under these assumptions, the following equations of continuity, momentum and energy have been found using boundary layer approximations, as

$$\frac{\partial(ru)}{\partial r}+\frac{\partial(rw)}{\partial z}=0, \tag{1}$$

$$\frac{\partial w}{\partial t}+u\frac{\partial w}{\partial r}+w\frac{\partial w}{\partial z}=\frac{\mu_{nf}}{\rho_{nf}}\left[\frac{1}{r}\frac{\partial}{\partial r}\left(r\frac{\partial w}{\partial r}\right)\right]-\frac{\sigma_{nf}}{\rho_{nf}}B_0^2 w \tag{2}$$

$$\rho_{nf}c_p\left(\frac{\partial T}{\partial t}+u\frac{\partial T}{\partial r}+w\frac{\partial T}{\partial z}\right)=-\nabla\cdot q+\mu_{nf}\left(\frac{\partial w}{\partial r}\right)^2+\frac{J^2}{\sigma_{nf}}. \tag{3}$$

Christov [3] and Han *et al.* [7] proposed that the heat flux equation satisfy the following relation

$$q+\lambda_1\left(\frac{\partial q}{\partial t}+V.\nabla\mathbf{q}+(\nabla\mathbf{V})q-q.\nabla\mathbf{V}\right)=-k\nabla\mathbf{T}, \tag{4}$$

Combining (3) and (4), leads to

$$\begin{aligned}
&\frac{\partial T}{\partial t}+u\frac{\partial T}{\partial r}+w\frac{\partial T}{\partial z}=\frac{\mu_{nf}}{\rho_{nf}c_p}\left(\frac{\partial w}{\partial r}\right)^2+\frac{k}{\rho_{nf}c_p}\left(\frac{\partial^2 T}{\partial r^2}+\frac{\partial^2 T}{\partial z^2}\right)+\frac{\lambda_1}{\rho_{nf}c_p}\left(\mu\frac{\partial}{\partial t}\left(\frac{\partial w}{\partial r}\right)^2\right.\\
&+u\frac{\partial}{\partial r}\left(\mu_{nf}\left(\frac{\partial w}{\partial r}\right)^2\right)+w\frac{\partial}{\partial z}\mu_{nf}\left(\frac{\partial w}{\partial r}\right)^2\bigg)+\frac{\lambda_1}{\rho_{nf}c_p}\bigg[-\rho_{nf}c_p\left(\frac{\partial^2 T}{\partial t^2}+\frac{\partial u}{\partial t}\frac{\partial T}{\partial r}+u\frac{\partial^2 T}{\partial r\partial t}\right.\\
&\left.+\frac{\partial w}{\partial t}\frac{\partial T}{\partial z}+w\frac{\partial^2 T}{\partial t\partial z}\right]-\rho_{nf}c_p u\frac{\partial}{\partial r}\left(\frac{\partial T}{\partial t}+u\frac{\partial T}{\partial r}+w\frac{\partial T}{\partial z}\right)-\rho_{nf}c_p w\frac{\partial}{\partial z}\left(\frac{\partial T}{\partial t}+u\frac{\partial T}{\partial r}+w\frac{\partial T}{\partial z}\right)\bigg]
\end{aligned} \tag{5}$$

subject to

$$\begin{aligned}
u=0,\quad w=U_w,\quad \frac{\partial T}{\partial r}=0\quad at\quad r=R,\\
w\to 0,\quad T\to T_\infty\quad as\quad r\to\infty,
\end{aligned} \tag{6}$$

The thermophysical properties of nanofluid terms occured in Eqn (5) are defined in [20, 21]. Moreover, the proposed work used the following thermophysical properties given in Table 1.

Table 1: Thermophysical properties of base fluid and Au nanofluid [22]

nps/ Base water	Density (kg/m^3)	Thermal conductivity $(W/m\ K)$	Specific heat $(J/kg\ K)$	Electric conductivity (S/m)
Au	19300	318	129	4.11×10^7
H_2O	997.1	0.613	4179	5.50

While, the values of viscosity coefficients $A_1,\ A_2$ and shape factor m of multi-shape nps are given in Table 2.

Table 2: Viscosity and shape factor of nps [23, 24]

	A_1	A_2	m
Platelet	37.1	612.6	5.72
Sphere	2.5	6.5	3.0

3 Dimensionless Model

Introducing the similarity variable as follows [25, 26]

$$\theta(\eta)=\frac{T-T_\infty}{T_\omega-T_\infty},\qquad \eta=\left(\frac{c}{\nu_f(1-\alpha t)}\right)^{\frac{1}{2}}\left(\frac{r^2-R^2}{2R}\right),\qquad \psi=\left(\frac{c\nu_f}{1-\alpha t}\right)^{\frac{1}{2}} zRf(\eta),\tag{7}$$

where the flow pattern ψ is defined as $u=-\frac{1}{r}\frac{\partial\psi}{\partial z}$ and $w=\frac{1}{r}\frac{\partial\psi}{\partial r}$, that satisfy the continuity equation (1) directly.
Using the similarity variables defined in (7), the momentum Eqn.(2) and energy Eqn.(5) with boundary condition (6) lead to

$$\epsilon_1(1+2\kappa\eta)f'''(\eta)+2\epsilon_1\kappa f''(\eta)+\left[f(\eta)f''(\eta)-f'^2(\eta)-S\left(f'(\eta)+\frac{\eta}{2}f''(\eta)\right)\right]-\epsilon_3 Mf'(\eta)=0,\tag{8}$$

$$\begin{aligned}\epsilon_1(1+2\kappa\eta)E_c f''^2(\eta)+\frac{\epsilon_1}{P_r}\Big(2\kappa\theta'(\eta)+(1+2k\eta)\theta''(\eta)\Big)+\beta_1\Big[(1+2\kappa\eta)\Big(3\epsilon_1 SE_c f''^2(\eta)+\\ \eta SE_c 3f''(\eta)f'''(\eta)-2E_c f(\eta)f''(\eta)f'''(\eta)+2E_c f'(\eta)f''(\eta)\Big)+2\epsilon_3 E_c M\Big(S(f'^2(\eta)+\frac{\eta}{2}f'(\eta)f''(\eta))\\ -f(\eta)f'(\eta)f''(\eta)+f'^3(\eta)\Big)-S^2\Big(6\theta(\eta)+\frac{11}{4}\eta\theta'(\eta)+\frac{\eta^2}{4}\theta''(\eta)\Big)+S\Big(5f(\eta)\theta'(\eta)+\eta f(\eta)\theta''(\eta)\\ -4f'(\eta)\theta(\eta)-\eta f'(\eta)\theta'(\eta)-f'(\eta)\theta(\eta)-\frac{\eta}{2}f''(\eta)\theta(\eta)\Big)+\frac{S}{2}\Big(f(\eta)\theta'(\eta)+\eta f'(\eta)\theta'(\eta)\Big)\\ +f(\eta)f''(\eta)\theta(\eta)-f'^2(\eta)\theta(\eta)-2\kappa E_c f(\eta)f''^2(\eta)-f^2(\eta)\theta''(\eta)+f(\eta)f'(\eta)\theta'(\eta)\Big]-\\ S\Big(2\theta(\eta)+\frac{\eta}{2}\theta'(\eta)\Big)+f(\eta)\theta'(\eta)-f'(\eta)\theta(\eta)+\epsilon_3 E_c M f'^2(\eta)=0,\end{aligned}\tag{9}$$

subject to

$$\begin{aligned}&f(\eta)=0,\quad f'(\eta)=1,\quad \theta(\eta)-1=0\quad at\quad \eta=0,\\ &f'(\eta)\to 0,\quad \theta(\eta)\to 0\quad as\quad \eta\to\infty.\end{aligned}\tag{10}$$

Where

- $\kappa = \frac{1}{R}\left(\frac{\nu_f(1-\alpha t)}{c}\right)^{\frac{1}{2}}$ is the Curvature parameter,
- $Ec = \frac{U_w^2}{C_p(T_w - T)}$ is the Eckert number,
- $M = \frac{\beta_0 \sigma_f (1-\alpha t)}{c\rho_{nf}}$ is the magnetic parameter,
- $Pr = \frac{(\rho\ C_p)_f\ \nu_f}{\kappa_f}$ is the Prandtl number,
- $S = \frac{\alpha}{c}$ is the unsteadiness parameter,
- $\beta_1 = \frac{c\lambda_1}{1-\alpha t}$ is the thermal relaxation parameter.

The constants $\epsilon_i,\ i = 1, \dots, 3$ are used in (8) and (9), defined in [27].
The rate of shear-stress and strain at the surface of vertically stretched cylinder can be written, as

$$C_f = \frac{2\mu_{nf}}{\rho_f\ U_w^2}\left[\frac{\partial u}{\partial r}\right]_{r=R}, \tag{11}$$

and

$$Nu = -\frac{z\kappa_{nf}}{\kappa_f\ (T_w - T_\infty)}\left[\frac{\partial T}{\partial r}\right]_{r=R}. \tag{12}$$

In non-dimensional form (11) and (12) can be written, as

$$\frac{1}{2}Re^{\frac{1}{2}}C_f = (1 + A_1\phi + A_2\phi^2)\ f''(0) \quad and \quad Re^{-\frac{1}{2}}Nu = -\frac{\kappa_{nf}}{\kappa_f}\ \theta'(0). \tag{13}$$

4 Method of Solution

This article uses the the BVP4C technique to solve the system (8-9) with boundary conditions (10). The following system of 1st-order ODE's is obtained by considering:

$$\begin{aligned}
f &= y_1, && (14)\\
y_1' &= y_2, && (15)\\
y_2' &= y_3, && (16)\\
y_3' &= \xi_1, && (17)\\
y_4 &= \theta, && (18)\\
y_4' &= y_5, && (19)\\
y_5' &= \xi_2, && (20)\\
y_4(\eta) - 1 &= 0, \quad y_1(\eta) = 0, \quad y_2(\eta) = 1, \quad at \quad \eta = 0, && (21)\\
y_2 &\to 0, \quad y_4 \to 0 \quad as \quad \eta \to \infty. && (22)
\end{aligned}$$

where

$$\xi_1 = \frac{1}{\epsilon_1(1 + 2\eta\kappa)}\left[\epsilon_3\ My_2 - 2\epsilon_1\kappa y_3 - \left\{y_1 y_3 - y_2^2 - S\left(y_2 + \frac{\eta}{2}y_3\right)\right\}\right], \tag{23}$$

and

$$\xi_2 = \frac{4Pr}{4\epsilon_1(1+2\kappa\eta) - Pr\beta_1\left(S^2\eta^2 - 4S\eta\, y_1 + 4y_1^2\right)}\Bigg[S\left(2y_4 + \frac{\eta}{2}y_5\right) - y_1y_5 + y_2y_4 - \left(\frac{2\kappa y_5\epsilon_1}{Pr}\right)$$
$$-(1+2\kappa\eta)\epsilon_1 Ec\; y_3^2 - \beta_1\bigg[(1+2\kappa\eta)\epsilon_1 sE_c(3y_3^2 + \eta y_3y_3') - 2\epsilon_1\kappa E_c y_1y_3^2 - 2(1+2\kappa\eta)\epsilon_1 E_c y_1y_3y_3'$$
$$+2(1+2\kappa\eta)\epsilon_1 E_c y_2y_3 - 6s^2y_4 - \frac{11}{4}s^2\eta y_5 + \frac{11}{2}sy_1y_5 - 5sy_2y_4 - \frac{\eta}{2}sy_2y_5 - s\frac{\eta}{2}y_3y_4$$
$$+2\epsilon_3E_cM(sy_2^2 + s\frac{\eta}{2}y_2y_3 - y_1y_2y_3 + y_2^3) + y_1y_2y_5 + y_1y_3y_4 - y_2^2y_4\bigg] - \epsilon_3E_cMy_2^2. \quad (24)$$

The obtained results of the proposed model are discussed in the following section in detail.

5 Results and Discussion

The primary aim of this article is to scrutinize the Cattaneo-Christov model within the context of Au nanofluid flow across a horizontally stretched cylinder. In this section, we embark on a comprehensive exploration of the impact of pertinent physical properties, leveraging illustrative graphical representations. Additionally, we prepared the numerical assessments of both skin friction and Nusselt number for each of nanoparticle, listed in Table 3 and 4. Graphical results are discussed below:

Figure 2 provides a visual representation of the influence of the thermal relaxation time parameter on multi-shaped nanoparticles (nps). For each distinct multi-shaped nps configuration, we observe a progressive elevation in the temperature field as the β_1 value is systematically adjusted. This phenomenon is fundamentally associated with the concept of β_1 serving as an indicator of the system's thermal responsiveness. As β_1 undergoes augmentation, it implies a decelerated response of the system to variations in temperature. This deceleration, in turn, has the potential to engender heightened temperature gradients, thereby fostering an increased rate of heat transfer.

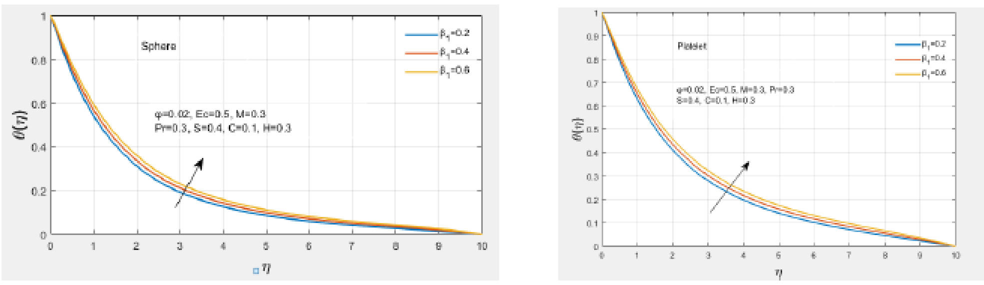

Figure 2: Effect of thermal relaxation time parameter β_1 on temperature profile

In Figure 3, we illustrate the influence of the Eckert number (Ec) on the temperature profile within a multi-shaped nanoparticles (nps) context. Notably, elevated values of the

Eckert number (Ec) are found to amplify the temperature profile across various multi-shaped nanoparticle scenarios. The Eckert number serves as a quantifier of the relative contribution of kinetic energy dissipation to the enthalpy difference within the boundary layer. At Ec $= 0$, no viscous dissipation is observed. However, as Ec increases, there is a progressively intensified conversion of kinetic energy into heat, manifesting as a pronounced elevation in temperature.

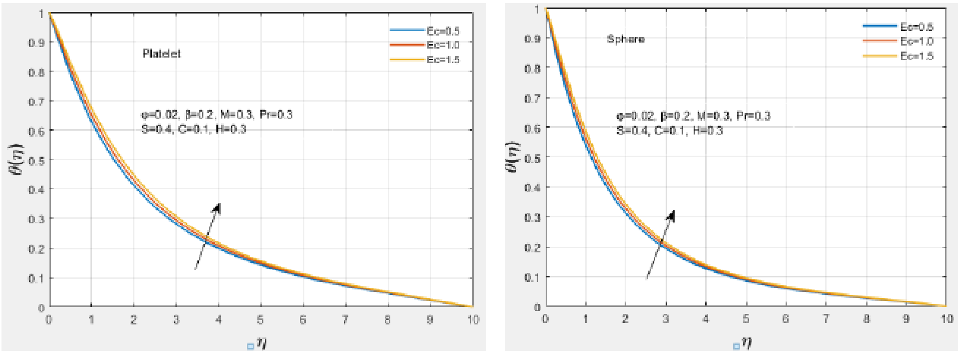

Figure 3: Effect of Eckert number on temperature profile

Figure 4 visually portrays the impact of the curvature parameter (κ) on the temperature profile within the context of multi-shaped nanoparticles (nps). Intriguingly, as the curvature parameter (κ) assumes higher values, we discern a consistent upward trajectory in the temperature field across various multi-shaped nanoparticle scenarios. In physical terms, higher values of the curvature parameter (κ) correspond to a reduction in the surface area of the cylinder, consequently leading to an augmentation in the boundary layer thickness. This structural transformation elucidates the observed increase in temperature.

Figure 4 visually portrays the impact of the curvature parameter (κ) on the temperature profile within the context of multi-shaped nanoparticles (nps). Intriguingly, as the curvature parameter (κ) assumes higher values, we discern a consistent upward trajectory in the temperature field across various multi-shaped nanoparticle scenarios. In physical terms, higher values of the curvature parameter (κ) correspond to a reduction in the surface area of the cylinder, consequently leading to an augmentation in the boundary layer thickness. This structural transformation elucidates the observed increase in temperature.

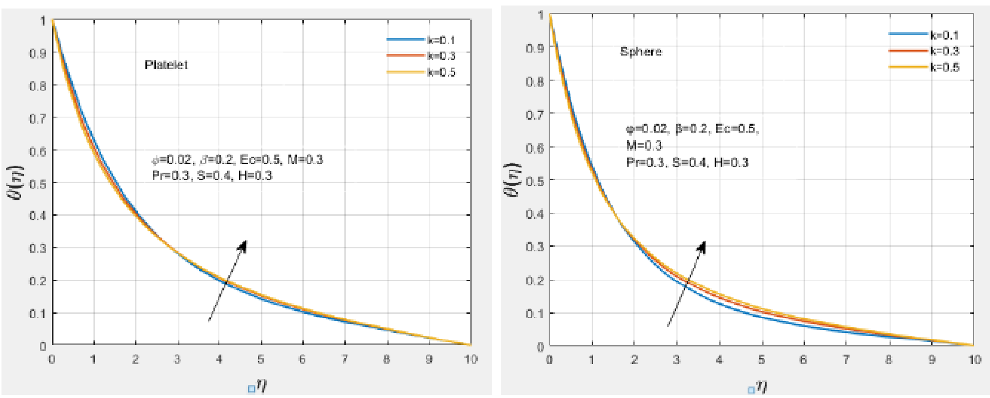

Figure 4: Effect of Curvature κ on temperature profile

The meticulous calculation of the skin friction coefficient, performed across various shapes of nanoparticles (nps), entails a systematic numerical exploration of the relevant physical parameters. A discernible trend emerges, characterized by a reduction in volume-fraction ϕ, magnetic field intensity M, and the unsteadiness parameter S for each distinct nps shape, as systematically documented in Table 3.

Table 3: Skin-friction coefficient of multi-shape nps

Physical	parameters		Platelet	Sphere
ϕ	M	S	$-Re^{\frac{1}{2}}C_f$	
0.02	0.3	0.4	2.1292944	1.5329756
0.04	-	-	3.1574166	1.7513594
0.06	-	-	4.3525226	1.9653005
0.02	**0.0**	0.4	1.9528047	1.4049071
-	**0.9**	-	2.4406545	1.7589701
-	**1.5**	-	2.7140426	1.9575569
0.02	0.3	**0.0**	1.9208778	1.3821864
-	-	**0.8**	2.3232968	1.6736942
-	-	**1.2**	2.5037787	1.8047596

Furthermore, the heat transfer rate exhibits a progressive augmentation in response to increasing values of volume-fraction ϕ, and Prandtl number and trend decreases for thermal relaxation as distinctly evidenced in Table 4.

Table 4: Nusselt number of multi-shape nps

Physical	parameters		Platelet	Sphere
ϕ	Pr	β	$Re^{-\frac{1}{2}}Nu$	
0.02	0.3	0.2	0.4227891	0.7341154
0.04	-	-	0.4622218	0.8027551
0.08	-	-	0.4653477	0.8578338
0.02	**0.2**	0.2	0.4431575	0.5500724
-	**0.4**	-	0.5894060	0.7397379
-	**0.5**	-	0.6471504	0.8131049
0.02	0.3	**0.0**	0.5810213	0.7407604
-	-	**0.4**	0.4659564	0.5696573
-	-	**0.6**	0.4103710	0.4866392

III. Conclusion

This article delves into the intricacies of heat transfer enhancements within the framework of the Cattaneo-Christov model, specifically applied to silica nanofluid flowing over a vertically stretching cylinder. Employing the BVP4C solver in MATLAB, we systematically unravel the nuances of this challenging problem. The crux of our findings is succinctly encapsulated in the following lines:

- The rate of heat transfer exhibits a negative correlation with the escalating values of the thermal relaxation time parameter, denoted as β_1.
- Meanwhile, the skin friction coefficient registers a declining trend concerning volume- fraction ϕ, magnetic field intensity M, and the unsteadiness parameter S.
- Additionally, the Nusselt number demonstrates an upsurge in response to increasing volume-fraction, and the prandtl number and decreases with the increase of thermal relaxation.

References

[1]. B. De. Fourier and J. B. Joseph, The Analytical Theory of Heat, The University Press, (1878).
[2]. C. Christov, On heat conduction, Atti Sem. Mat. Fis. Univ. Modena Reggio Emilia, 3 (1948) 83-101.
[3]. C. I. Christov, On frame indifferent formulation of the Maxwell–Cattaneo model of finite-speed heat conduction, Mechanics Research Communications, 36 (4) (2009) 481- 486.
[4]. B. Straughan, Thermal conductive with Cattaneo-Christov model, International Journal of Heat and Mass Transfer, 53 (2010) 95-98.
[5]. M. Ciarletta and B. Straughan, Uniqueness and structural stability for the Cattaneo– Christov equations, Mechanics Research Communications, 37 (5) (2010) 445-447.
[6]. V. Tibullo and V. Zampoli, A uniqueness result for the Cattaneo–Christov heat con- duction model applied to incompressible fluids, Mechanics Research Communications, 38 (1) (2011) 77-79.
[7]. S. Han, L. Zheng, C. Li and X. Zhang, Coupled flow and heat transfer in viscoelastic fluid with Cattaneo–Christov heat flux model, Applied Mathematics Letters, 38 (2014) 87-93.
[8]. O. D. Makinde, V. Nagendramma, C. S. K. Raju, and A. Leelarathnam, Effects of Cattaneo-Christov heat flux on Casson nanofluid flow past a stretching cylinder, In De- fect and Diffusion Forum, 378 (2017) 28-38.

[9]. S. M. Upadhya, Mahesha and C. S. K. Raju, Cattaneo-Christov heat flux model for magnetohydrodynamic flow in a suspension of dust particles towards a stretching sheet,Nonlinear Engineering, 7 (3) (2018) 237-246.
[10]. M. khan, A. Ahmed, M. Irfan and J. Ahmed, Analysis of Cattaneo-Christov theory for unsteady flow of Maxwell fluid over stretching cylinder, Journal of Thermal Analysisand Calorimetry, 144 (2021) 145-154.
[11]. Z. Elahi, M. T. Iqbal and A. Shahzad, Numerical Simulation of Heat Transfer Devel- opment of Nanofluids in a Thin Film over a Stretching Surface, Brazilian Journal of Physics, 52 (2) (2022) 1-13.
[12]. R. Ali, A. Shahzad, K. Saher, Z. Elahi and T. Abbas The thin film flow of Al_2O_3 nanofluid particle over an unsteady stretching surface, Case Studies in Thermal Engi-neering, 29 (2022) 101-695.
[13]. J. Ahmed, A. Begum, A. Shahzad and R. Ali, MHD axisymmetric flow of power-law fluid over an unsteady stretching sheet with convective boundary conditions, Results in Physics, 6 (2016) 973-981.
[14]. J. Ahmed, A. Shahzad, A. Begum, R. Ali and N. siddiqui Effects of inclined Lorentz forces on boundary layer flow of Sisko fluid over a radially stretching sheet with radiative heat transfer, Journal of the Brazilian Society of Mechanical Sciences and Engineering, 39 (8) (2017) 3039–3050.
[15]. A. Shahzad, R. Ali, A. Begum, M. Hussain and M. Kamran Unsteady axisymmetric flow and heat transfer over time-dependent radially stretching sheet, Alexandria EngineeringJournal, 56 (1) (2017) 35-41.
[16]. J. Ahmed, A. Shahzad K. Masood and R. Ali, A note on convective heat transfer of an MHD Jeffrey fluid over a stretching sheet, American Institute of Physics advances,5 (11) (2015) 117.
[17]. A. M. Alqahtani, M. Bilal, F. A. Z. Elsebaee, S. M. Eldin, T. R. Alsenani and A. Ali, Energy transmission through carreau yasuda fluid influenced by ethylene glycol with activation energy and ternary hybrid nanocomposites by using a mathematical model, Heliyon, 9 (4) (2023).
[18]. A. M. Alqahtani, M. Bilal, A. Ali, T. R. Alsenani and S. M. Eldin, Numerical solution of an electrically conducting spinning flow of hybrid nanofluid comprised of silver and gold nanoparticles across two parallel surfaces, Scientific Reports, 13 (1) (2023) 7180.
[19]. S. Murtaza, P. Kumam, M. Bilal, T. Sutthibutpong, N. Rujisamphan and Z. Ahmed, Parametric simulation of hybrid nanofluid flow consisting of cobalt ferrite nanoparticles with second-order slip and variable viscosity over an extending surface, NanotechnologyReviews, 12 (1) (2023) 20220533.
[20]. F. A. A. Elsebaee, M. Bilal, S. R. Mahmoud, M. Balubaid, M. Shuaib, J. K. K. Asamoah, and A. Ali, Motile micro-organism based trihybrid nanofluid flow with an application of magnetic effect across a slender stretching sheet: Numerical approach, American Institute of Physics Advances, 13 (3) (2023) 035237.
[21]. T. A. Assiri, F. A. A. Elsebaee, A. M. Alqahtani, M. Bilal, A. Ali, and S. M. Eldin, Numerical simulation of energy transfer in radiative hybrid nanofluids flow influenced by second-order chemical reaction and magnetic field, American Institute of Physics Advances, 13 (3) (2023) 035020.
[22]. A. M. Alqahtani, M. Bilal, M.Usman, T. R. Alsenani, A. Ali and S. R. Mahmuod, Heat and mass transfer through MHD Darcy Forchheimer Casson hybrid nanofluid flow across an exponential stretching sheet, ZAMM-Journal of Applied Mathematics and Mechanics/Zeitschrift für Angewandte Mathematik und Mechanik, (2023) e202200213.
[23]. H. Khalil, T. Zahra, Z. Elahi and A. Shehzad, Effect of Titanium Oxide Nanofluid over Cattaneo-Christov Model, (Functional Calculus-Recent Advances and Development) (2022).
[24]. A. Ali, S. Sarkar, S. Das, J. Sanatan and R. Nath Investigation of cattaneo– christov double diffusions theory in bioconvective slip flow of radiated magneto-cross- nanomaterial over stretching cylinder/plate with activation energy, International Jour- nal of Applied and Computational Mathematics, 7 (5) (208) 2021.
[25]. N.V. Ganesh, B. Ganga, A. K. A. Hakeem, S. Sarayna and R. Kalaivanan, Hydro- magnetic axisymmetric slip flow along a vertical stretching cylinder with a convective boundary condition, St. Petersburg State Polytechnical University Journal. Physics and Mathematics, 4 (2016) 253.
[26]. S. Shah, S. Hussain, M. Sagheer, MHD effects and heat transfer for the UCM fluid along with Joule heating and thermal radiation using Cattaneo-Christov heat flux model, Aip Advances, 6 (8) (2016).
[27]. Reddy, R. Gnaneswara , S. Kumar, G.Prasannakumar, B. Chamkha, J. Ali, Cattaneo– Christov heat flux model on Blasius–Rayleigh–Stokes flow through a transitive magnetic field and Joule heating, Physica A: Statistical Mechanics and its Applications, 548, (123991), (2020).